Buoyancy-driven motions in particle-laden fluids

By HERBERT E. HUPPERT

Institute of Theoretical Geophysics, 20 Silver Street, Cambridge CB3 9EW, UK.

Many fluid flows, in both natural and industrial situations, are driven by the suspended particles in the fluid. This paper briefly reviews a number of such flows. The convective overturn that occurs when a suspension layer of small heavy particles is heated from below is described and quantified. Results from laboratory experiments, which are in good agreement with the theoretical predictions, are discussed. A description is given of the convective mixing that arises when a clear fluid layer overlies a suspension layer with the density of the upper layer intermediate between that of the interstitial fluid and the bulk density of the lower layer. The interface between the two layers is shown to descend at a constant rate which is much more rapid than if the upper layer was absent. The effects of adding a forced turbulent flow to the lower layer are also described. A unifying theme which runs throughout the paper is the recognition that the slow descent of small heavy particles at low Reynolds number can lead to large-scale convective motions at intrinsically high Reynolds numbers.

1. Preliminary remarks

The large-scale motion of a fluid which contains suspended particles is a frequent occurrence in many natural and industrial situations. Examples include: the smog layer which is now seen almost continuously off La Jolla and which emanates from Los Angeles; turbidity currents in the ocean; haboobs which are initiated over hot deserts; snow avalanches; and the sludge outflows from many industrial plants. In numerous situations the particles act merely as passive tracers and do not affect the flow directly. Recently I have become interested in flows for which the actual presence of particles is essential. In this paper I will briefly bring out the highlights of some of my current research in this area.

A few introductory remarks about the suspension of particles in *steady* two-dimensional flows will be followed by a discussion of particle motions in turbulent flows. A series of experiments that we have conducted in this area, and the theoretical interpretation of them, will be discussed in §2. The next section will consider the fate of a fluid layer which suspends a polydisperse distribution of small heavy particles and above which is placed a clear fluid layer, where the densities are arranged such that the density of the upper layer lies between the density of the interstitial fluid and the bulk density of the lower layer. Vigorous convective motions are generated above the interface as the relatively light interstitial fluid rises into the upper layer, and the interface descends at a constant velocity. This velocity can be considerably larger than that if the upper layer is absent, but because particles are entrained by the convective motions into the upper layer the time taken for complete sedimentation can be considerably increased. The penultimate section will describe rather briefly some preliminary experiments and related theory that I am currently

working on with Stewart Turner and Mark Hallworth on the effect of mechanically stirring the lower layer with a mixing grid. A few tentative conclusions will be drawn together in the final section.

An early investigation of particle-laden fluid motions was carried out by Stommel (1948). He considered whether small heavy particles could remain suspended indefinitely in a steady two-dimensional flow with closed streamlines, such as a two-dimensional Bénard roll. Even today his results are not well known by the general fluid dynamical community, despite the concepts having been rederived, to some extent independently, by others (see, for example, Merry & Davidson 1973; Marsh & Maxey 1985; Weinstein, Yuen & Olsen, 1988 and also Huppert 1984 for the results of an amusing survey investigating knowledge on this point).

Consider the fluid flow to be specified by the sufficiently smooth stream function $F\psi_f$ so that with respect to horizontal and vertical axes x and z respectively, the horizontal and vertical velocities, u and w, are given by

$$q \equiv (u, w) = F(\partial_z \psi_f, -\partial_x \psi_f), \tag{1.1a,b}$$

where ψ_f has been normalized so that

$$\max \mid \nabla \psi_f \mid = 1 \tag{1.2}$$

with the maximum taken over the flow domain. Thus F represents the maximum velocity in the flow. Let the Stokes velocity of each particle in a quiescent fluid be v_S, which is assumed to be independent of the presence of any other particles. Then the stream function ψ_p describing the motion of the particles is given by

$$\psi_p = F\psi_f + v_S x. \tag{1.3}$$

Thus

$$\nabla \psi_p = F[\nabla \psi_f + S(1, 0)], \tag{1.4}$$

where the Stommel number

$$S = v_S / F \tag{1.5}$$

is the ratio of the free fall velocity to the maximum fluid velocity. Because streamlines of the pure fluid flow are closed curves, $\nabla \psi_f = 0$ somewhere in the flow field, and thus, for sufficiently small $S, \nabla \psi_p$ is also zero somewhere. Some of the particle streamlines must hence also be closed; that is, for sufficiently small S some particles will remain in suspension indefinitely.

To evaluate the region to which the particles are bounded, and also its variation with S requires ψ_f to be specified and (generally) numerical calculation. Stommel (1948) carried out such a calculation for $\psi_f = \sin \pi x \sin \pi z$. Figure 1 shows the fluid streamlines and particle trajectories for S = 0.5. The stippled region, in which the particles are maintained in suspension, occupies one-third of the total area for this value of S and decreases monotonically to 0 as S increases to 1.

In their investigations of crystal motions in magma chambers, Huppert & Sparks (1980) considered the motion of small dense particles in an intensely turbulent flow. Equating the upward turbulent transport flux to the downward concentration flux, they argued that a steady-state particle concentration $C(z)$ would be set up of the form

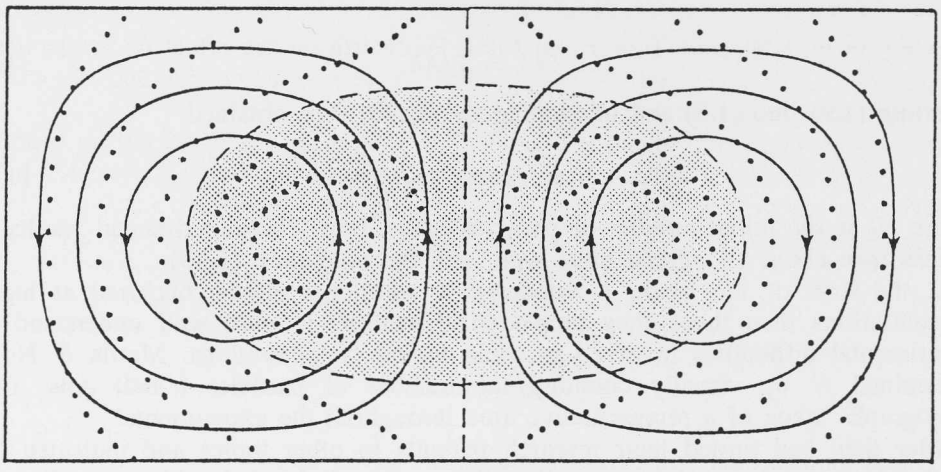

FIGURE 1. Fluid streamlines (——) and particle streamlines (.....) for the steady two-dimensional fluid flow described by $\psi_f = \sin \pi x \sin \pi z$ with the Stommel number $S \equiv v_S/F = 0.5$, where v_S is the intrinsic Stokes velocity of the particles and F is the maximum velocity of the fluid. Particles in the stippled region follow closed streamlines and remain in suspension indefinitely. (The curves have been adapted from figure 2 of Marsh & Maxey 1985.)

$$C(z) = C_0 \exp(-S_t z/h), \tag{1.6}$$

where C_0 is the particle concentration at the base of the layer of height h and the turbulent Stommel number

$$S_t = v_S/W, \tag{1.7}$$

where W is the root-mean-square vertical velocity at the mid-depth of the layer. Determining W *qua* function of the buoyancy flux from previous work (Townsend 1976 and Deardorff & Willis 1967), Huppert & Sparks (1980) found that for the system they were considering $S_t \ll 1$. They hence argued that strong turbulent motions kept all the particles in suspension with an almost uniform concentration.

I can report here that Sparks was slightly unhappy about this conclusion at the time. He wondered about the effect of the lower boundary layer and whether particles might not be lost to the flow because of the low velocity there. I replied in rather vague phrases like: small mean flows but relatively large fluctuations at the bottom; saltation; S_t was so very large, etc.

Our results became well known to the geological community, though they were not uncritically accepted. Showing a healthy scepticism of our ideas, Martin & Nokes (1988, 1989) carried out a series of experiments at the Australian National University in which polystyrene particles at very low concentrations were initially placed uniformly throughout a fluid-filled box in which turbulent convection was driven by cooling the box from above. They found that the number of particles N remaining in suspension gradually decreased with time. They argued that particles fall out to the base of the container, of area A, at a rate given by

$$\frac{dN}{dt} = -Av_S C_0. \tag{1.8}$$

For large S_t the particle concentration is nearly uniform throughout the interior of the box, and so

$$C_0 = N/Ah. \tag{1.9}$$

Inserting (1.9) into (1.8) and integrating the result, they obtained

$$N = N_0 \exp(-v_S t/h), \tag{1.10}$$

where N_0 is the initial number of particles in the box. The experimental results for S_t less than about 0.5 agreed quite well with the prediction (1.10).

At the time of the work, I wondered if additional effects occurred at higher concentrations than those they employed. However, I could well understand the experimental difficulties involved in using higher concentrations: Martin & Nokes determined N by visually counting the number of particles (small dots) from photographs taken of a representative area throughout the experiments!

After they had turned their research pursuits to other topics and indicated that they were not interested in extending their work, I decided with my colleagues at Cambridge to investigate the matter further. Our work on flows with higher concentrations which are driven by either heating from below or cooling from above (but not yet both) are described in the next section.

2. Convective overturn at moderate concentrations

The experiments and related theory of Martin & Nokes (1988, 1989) which were described in the last section were based on such small particle concentrations that their presence had no influence on the background convective motions of the fluid. In order to overcome this constraint, we conducted a series of experiments in a 20 $\times$ 20 $\times$ 20 cm tank either heated from below or cooled from above (Koyaguchi *et al.* 1990). The tank was filled with water laden with relatively well-sorted silicon carbide grinding powder (carborundum). The irregularly shaped particles have a density of 3.217 g cm^{-3} and a medium diameter of 16 μm with a standard deviation of about 3 μm. The Stokes free-fall velocity, v_S, of such small particles in water is of order 0.02 – 0.04 cm s^{-1}, which implies that the particle Reynolds number is of order 10^{-3}. The initial temperature differences between the fluid and the heated or cooled surface was typically between 5 and 15^{0}C, which implies that the initial Rayleigh number was of order 10^9. The suspension was well mixed at the start of each experiment and then left to evolve. Temperature and particle concentration data were obtained at several heights in the tank using thermistors and a specially designed and built optical transmission device respectively. Our experiments concentrated mainly on the situation of heating from below since the behaviour in this situation is more interesting; and we shall emphasize this situation hereinafter.

At very low initial concentrations (less than about 0.003 vol.%), the particles remained distributed fairly uniformly throughout the tank during an experiment, while a sediment layer built up exponentially with time at the base. All this is in agreement with the experiments and related theory of Martin & Nokes (1988, 1989). However, at higher, but still quite low, initial particle concentrations a totally different behaviour was observed (figure 2). The particles settled through a convecting lower layer leaving behind a clear fluid upper layer. These two layers were separated by an interfacial zone (figure 2b, c) due to the (unfortunate) polydisperse distribution of the particles. The interfacial zone descended at approximately the Stokes settling velocity, during which time particles sedimented at the base of the tank and the mean temperature of the lower layer gradually increased.

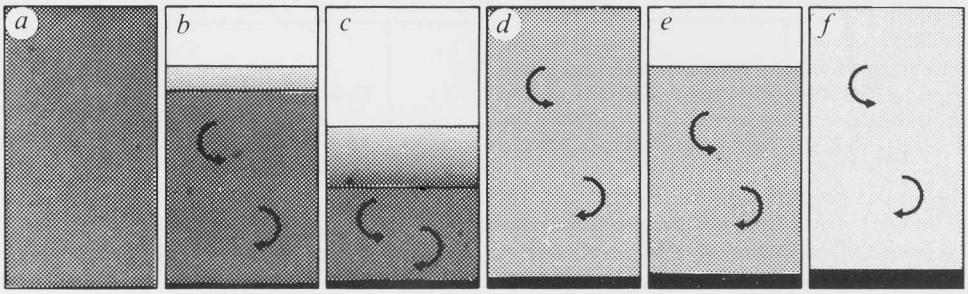

FIGURE 2. A schematic sketch of small heavy particles sedimenting through a fluid layer which is turbulently convecting owing to being heated from below. The details of the motion are described in the text.

After some time the lower layer abruptly overturned into the upper layer and the fluid in the tank returned to its initial, well-mixed state, except for the layer of sediment on the base (figure 2d). The cycle could be repeated several times (figure 2e, f) with a smaller particle concentration in the fluid after each overturn. The time interval between overturns decreased with each successive overturn. Eventually, both the particle concentration and the temperature difference between the fluid and the base became sufficiently low that the behaviour reverted to the previously described exponential deposition of particles from a suspension of uniform temperature and concentration. A movie sequence of an experiment was taken and part of it shown during the John Miles Symposium. The cause of the overturn is the decrease in density of the lower layer due to the heat flux at the base. Eventually the negative thermal contribution to the density of the lower layer overcomes the positive contribution due to the particles, and the bulk density of the lower layer is no longer greater than that of the upper layer.

Based on the experimental observations, we developed a simple physical model of the phenomenon. For simplicity, we assume that the particles are all of one size and that the resulting interfacial zone is of zero thickness. The evolving lower layer is assumed to convect due to a fixed temperature T_B at the base with the heat flux, Q, from the base given by the well known four-third's law (Turner 1979)

$$Q = \rho c \gamma (\alpha g \kappa^2 / \nu)^{1/3} (T_B - T_L)^{4/3}, \tag{2.1}$$

where ρ is the fluid density, c its specific heat, α its coefficient of thermal expansion, κ its thermal diffusivity, ν its kinematic viscosity, g the acceleration due to gravity, T_L the temperature of the lower layer and γ is a dimensionless constant which has been determined empirically to be about 0.1 at high Rayleigh numbers (Denton & Wood 1979). Note that in writing down (2.1) we have assumed that the particle concentrations are sufficiently low that they do not affect either the heat transfer rate or the value of any of the physical parameters of the fluid, such as viscosity or specific heat.

The governing equations are obtained by considering the change in heat contents of the upper and lower layers over a small time interval δt during which time the top of the particles settle at velocity v_S while the warm fluid left behind mixes with the upper layer (figure 3). Using the notation shown in figure 3, we see that for the upper layer

$$h_U T_U + \delta h_U T_L = (h_U + \delta h_U)(T_U + \delta T_U), \tag{2.2}$$

which in the limit $\delta t \to 0$ becomes

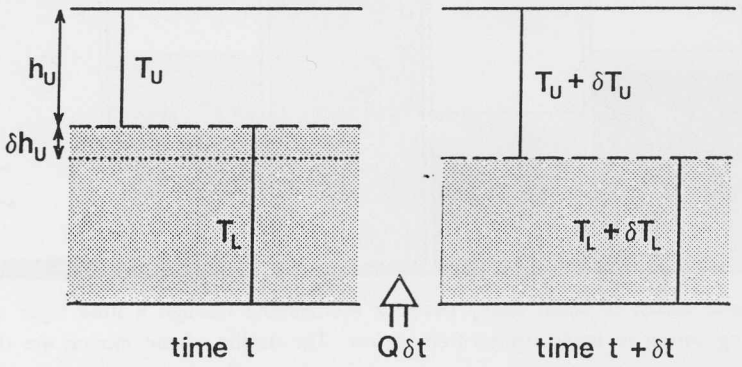

FIGURE 3. A schematic sketch of the changes in time δt of the temperatures of the upper and lower layers, T_U and T_L respectively, and the height of the upper layer h_U. A small amount of lower layer fluid of thickness δh_U and at temperature T_L is cleared of particles and mixes with fluid of the upper layer during this time.

$$\frac{d}{dt}(h_U T_U) = \frac{dh_U}{dt} T_L. \tag{2.3}$$

In a similar fashion the governing equation for the lower layer is

$$(H - h_U)\frac{dT_L}{dt} = Q/\rho c, \tag{2.4}$$

or

$$(H - v_S t)\frac{dT_L}{dt} = \gamma\left(\frac{\alpha g \kappa^2}{\nu}\right)^{1/3}(T_B - T_L)^{4/3}, \tag{2.5}$$

where H is the total depth of the two layers. The two initial conditions required to solve (2.4) and (2.5) are

$$T_U = T_L = T_0 \qquad (t = 0), \tag{2.6}$$

where T_0 is the initial temperature of both layers.

Equations (2.2) – (2.6) are only valid until either $t = H/v_S$, at which time particles will have totally sedimented *without* the lower layer having overturned, or until the time, say t_*, at which the bulk density of the lower layer first equals that of the upper layer. A relationship for the bulk density, ρ_L, of the lower layer is derived by considering the contributions made by the particles and fluid separately to obtain

$$\rho_L = [C\rho_p^{-1} + (1 - C)\rho_f^{-1}]^{-1}, \tag{2.7}$$

where C is the particle concentration expressed as a mass fraction ρ_p is the density of the particles and $\rho_f(T_L)$ is the density of the interstitial fluid of the lower layer *qua* function of its temperature. Representing this function as

$$\rho_f = \rho_0[1 - \alpha(T_L - T_0)], \tag{2.8}$$

employing a similar expression for the density of the upper layer, and expanding (2.7) for $C \ll 1$, we can show that the condition for overturn is

$$T_L - T_U = C(\rho_p - \rho_0)/(\alpha\rho_p). \tag{2.9}$$

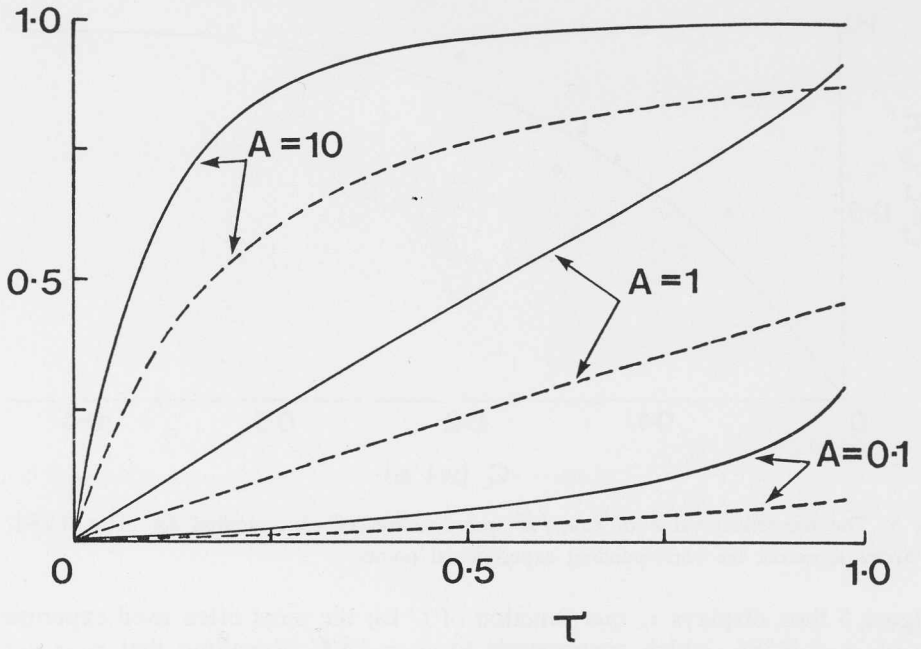

FIGURE 4. The theoretical non-dimensional temperatures of the upper (- - - - -) and lower (——) layers as functions of the non-dimensional time τ for A = 0.1, 1.0 and 10.0.

Introducing the non-dimensional variables

$$\theta_U = (T_U - T_0)/\Delta, \qquad \theta_L = (T_L - T_0)/\Delta \qquad \text{and} \qquad \tau = v_S t/H, \qquad (2.10a,b,c)$$

where $\Delta = T_B - T_0$ into (2.4) – (2.6) and (2.9), we obtain the nondimensional governing equations

$$\tau \frac{d\theta_U}{d\tau} + \theta_U - \theta_L = 0 \qquad (2.11)$$

$$(1-\tau)\frac{d\theta_L}{d\tau} = A(1-\theta_L)^{4/3} \qquad (2.12)$$

$$\theta_U = \theta_L = 0, \qquad (\tau = 0) \qquad (2.13a,b)$$

where

$$A = \gamma v_S^{-1}(\alpha \Delta g \kappa^2/\nu)^{1/3}, \qquad (2.14)$$

which are valid for

$$0 < \tau < \min(1, \tau_*), \qquad (2.15)$$

where τ_* is the time at which

$$\theta_L - \theta_U = C(\rho_p - \rho_0)/(\alpha \Delta \rho_p). \qquad (2.16)$$

While it is straightforward to obtain a closed-form analytic solution of (2.12) and (2.13b) which can then be substituted into (2.11) and (2.13a) to obtain a solution for θ_U in terms of exponential integrals, it is easier these days to obtain numerical solutions of (2.11) – (2.13) using standard packages. The results of such a procedure are shown in figure 4 which presents graphs of $\theta_U(\tau)$ and $\theta_L(\tau)$ for three values of

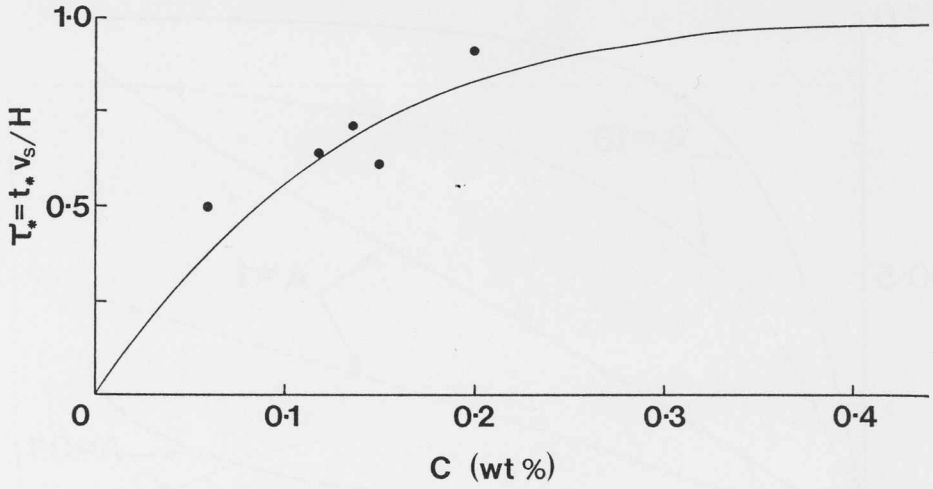

FIGURE 5. The theoretical value of $t_* v_S/H$ *qua* function of concentration for $A = 0.284$. The solid circles represent the corresponding experimental points.

A. Figure 5 then displays τ_* *qua* function of C for the most often used experimental value of $A = 0.284$, which corresponds to $\Delta = 15^0$C. Recalling that $\tau_* = v_S t_*/H$ is the ratio of the time for the lower layer to overturn to the time for the particles to settle to the base of the tank, we see that for very small C no matter what the value of A the timescale for the overturn is short compared to the settling time, and on this latter timescale the overturn appears to occur almost continuously. This is in agreement with the concepts and experiments presented by Martin & Nokes (1988, 1989). For larger, but still quite small, values of C the overturning takes place before the particles have sedimented to the base. A critical value of C is reached beyond which $\tau_* = 1$ and no overturning takes place. The theoretical results obtained using the mean Stokes velocity of 0.03 cm s^{-1} are seen to agree well with the experimental data, despite the polydisperse nature of the particles employed. Nevertheless, we hope to repeat the experiments with more uniform particles in the future.

3. Convection and particle entrainment due to polydisperse sedimentation

While I was visiting the Australian National University late in 1988, Stewart Turner and I started an investigation in which we were later joined by Ross Kerr and John Lister. The question we posed was as follows. How does a well-mixed suspended layer of small heavy particles behave if it is overlain by a large clear fluid layer whose density ρ_U lies between that of the interstitial fluid of the lower layer ρ_I and its bulk density ρ_B? Such a situation can arise when a silt-laden fresh water river intrudes into a salt-water environment. Other examples include the flow of hot, ash-laden pyroclastic flows in the atmosphere and the settling of crystals in light released magma in a magma chamber.

After a number of false starts, we carried out a series of experiments with two types of carborundum grinding powders whose size distributions are graphed in figure 6. Most of the experiments were carried out in a Perspex tank which consisted of a working section 19.5 × 3 × 20 cm high joined at its top to the base of a very much larger region which was 19.5 × 40 × 20 cm high, as sketched in figure 7. This large region allowed the experiment to continue without any significant change in the properties of the upper layer. An experiment was commenced by pouring an

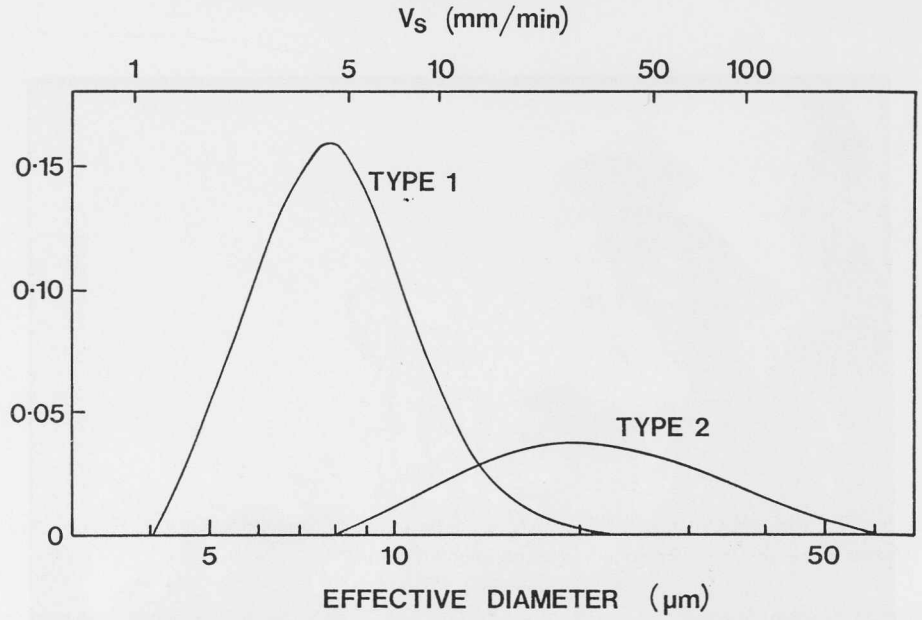

FIGURE 6. The distribution of particle sizes of the two batches of carborundum that we used to investigate effects of polydisperse sedimentation. The effective diameter is the diameter of the small spherical carborundum particles that would have the same settling velocity. Also shown are these settling velocities in water.

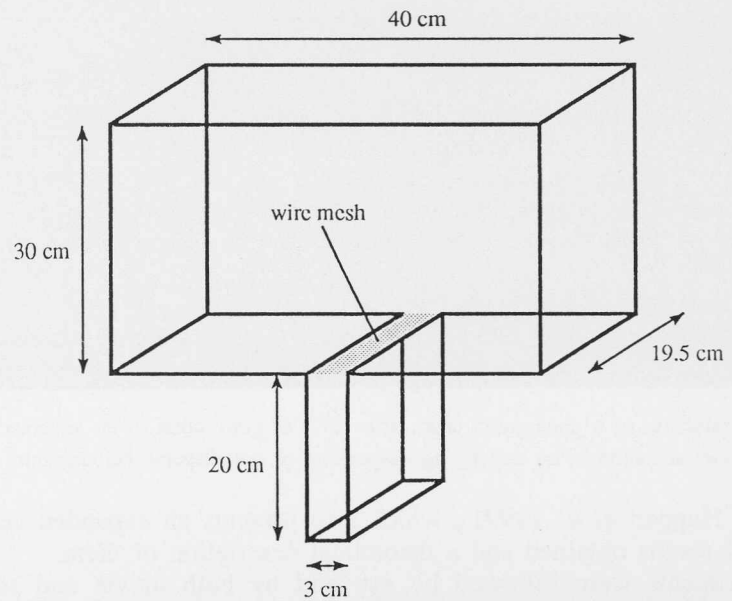

FIGURE 7. The Perspex tank used for most of the experiments on polydisperse sedimentation. The wire mesh helped shield the convective motions in the lower region from the large-scale circulation in the upper region.

aqueous sugar solution of known density into the tank. The more dense suspension layer was then added under the sugar solution by the use of a long vertical pipe emanating from the base of a continuously stirred reservoir. Further details are to

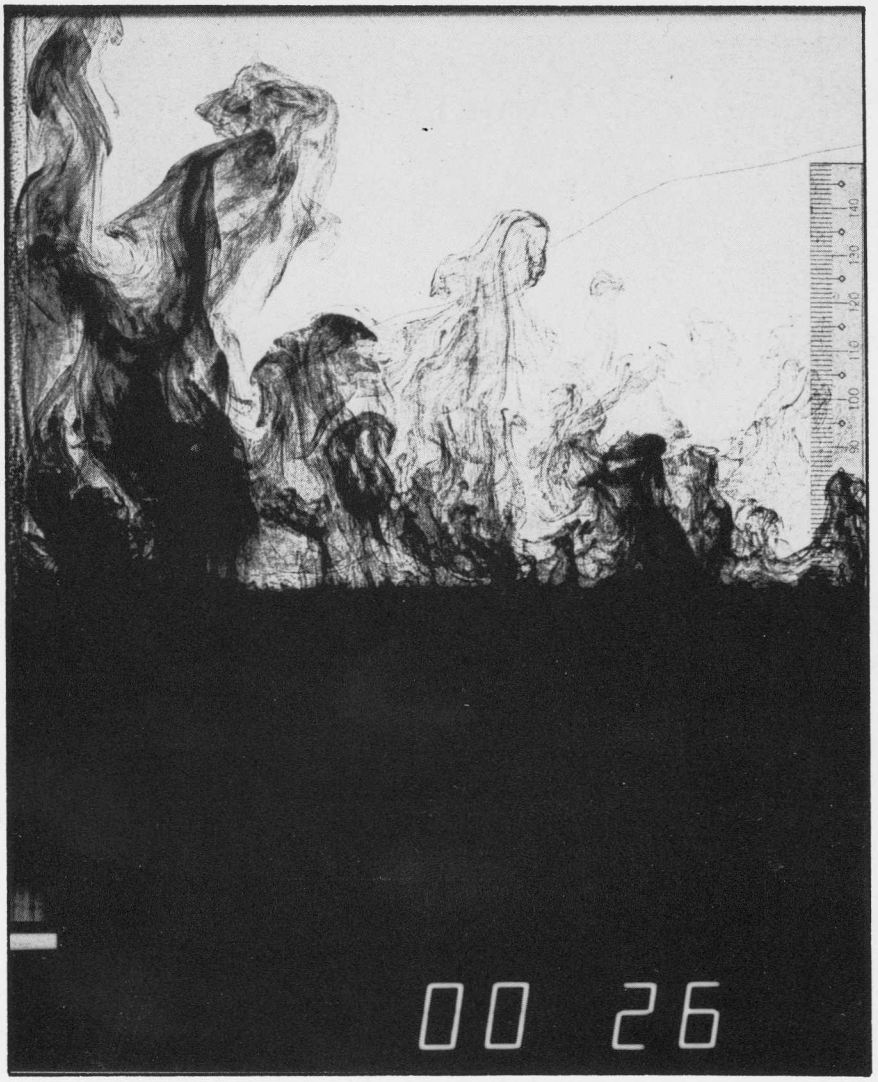

FIGURE 8. Reproduction of a photograph taken after 26 s of convection in an aqueous sugar solution driven by the sedimentation in an underlying suspension of polydisperse carborundum in pure water.

be found in Huppert *et al.* (1991), which also presents an expanded version of the experimental results obtained and a theoretical description of them.

The experiments were followed by eye and by both movie and still cameras. A sequence of the movie was shown during the Symposium and a typical frame is reproduced in figure 8. As the particles settled in the lower layer, buoyant interstitial fluid was left behind, which rose in thin streamers and sheets and carried with it some of the suspended particles. There was vigorous convection in the upper layer, which extended all the way to the top of the large tank. Careful observations with a microscope revealed that below a sharp interface the particles fell vertically with little additional motion in the lower layer. The experiments thus combined

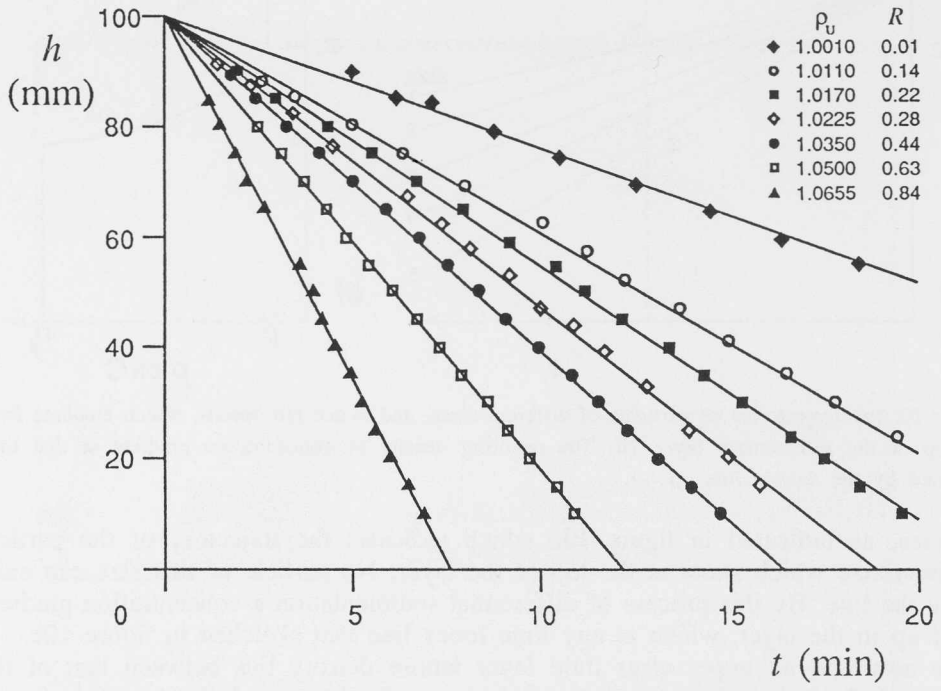

FIGURE 9. The measurements of interfacial height *qua* function of time for experiments which used type-1 particles so that the bulk density of lower layer, ρ_B, was initially 1.079 g cm^{-3}. The experiments were conducted at various values of the density of the upper layer ρ_U. Also shown is the value of the dimensionless ratio $R = (\rho_U - \rho_I)/(\rho_B - \rho_I)$, where ρ_I is the density of the interstitial fluid, here (pure) water. The data shows both that the interfacial velocity is essentially constant during an experiment and that it is a monotonically increasing function of R.

sedimentation at low Reynolds number in the lower layer of ever decreasing depth with convection at high Reynolds number in the upper layer.

The level of the interface between the two layers was recorded *qua* function of time. The results for various densities of the upper layer with a fixed bulk density of the lower layer are presented in figure 9. It was noted that in each experiment (and not just the ones presented in figure 9) the interface fell at a constant velocity, which systematically increased as the density of the upper layer increased (with all other variables held fixed).

Measurements of the refractive index of the interstitial fluid of the lower layer throughout an experiment confirmed that no sugar was transported into the lower layer, while measurements of the sediment content revealed that the local concentration of the particles decreased monotonically with time. This decrease at any point, as well as the rate of accumulation at the base, was shown to be independent of the presence of the upper layer.

The explanation of all these observations is as follows. Consider first a single layer of initially well-mixed polydisperse heavy particles. Each particle will fall through the layer at its own Stokes free-fall velocity, diminished by all the effects of particle-particle interactions. In this physical description we shall ignore the latter interactions since they are typically small and do not affect the essential aspects of the motion. (These interactions are, however, discussed and included in Huppert *et al.* 1991). The larger particles will fall more rapidly and leave behind the smaller

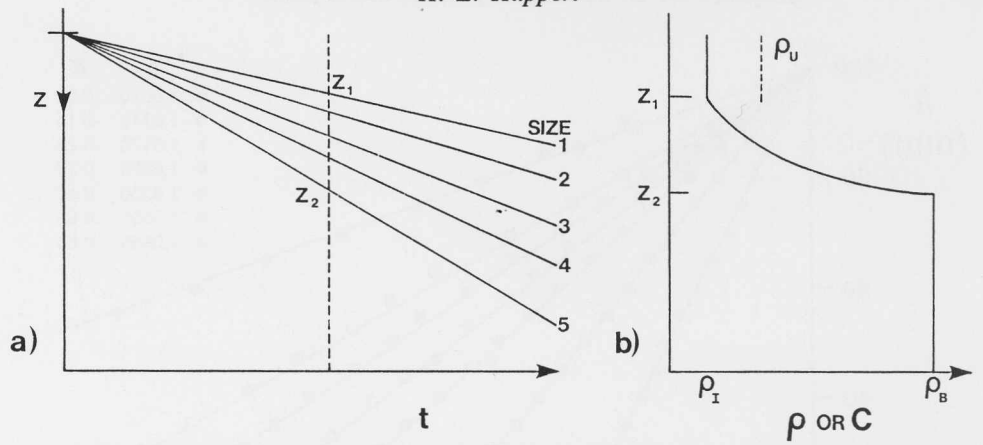

FIGURE 10. (a) Trajectories of particles of different sizes, and hence fall speeds, which emanate from the top of the sedimentary layer. (b) The resulting density or concentration gradient at that time indicated by the dashed line on (a).

particles, as indicated in figure 10a which indicates the trajectory of the particle of given size which starts at the top of the layer. No particle of this size can exist above the line. By this process of differential sedimentation a concentration gradient is set up in the layer, which at any time looks like that sketched in figure 10b.

We now add an upper clear fluid layer whose density lies between that of the interstitial fluid and the initial or maximum bulk density of the lower layer, as indicated on figure 10b. The initial sedimentation will be as just described, with a region near the top of the lower layer, whose thickness grows linearly with time, which is less dense than the overlying fluid. When a local Rayleigh number based on the unstable stratification and the increasing thickness of this region becomes sufficiently large, the region will rise and mix convectively with the overlying fluid and may also take some of the underlying suspension with it. The essentials of the process are similar in concept to those suggested by Howard (1966) in his famous paper modelling the instability of an evolving thermal boundary layer from a heated horizontal surface. Just as Howard envisaged a series of repeated detachments, so we envisage that the process we have just described continues to repeat itself. An unstable region develops at the top of the sedimenting layer, in which the rate of fall of the individual particles has been unaffected by the previous unstable processes. After a certain time this region rises into the upper layer and the cycle is repeated yet again. The period of each cycle is very short compared to the timescale of the sedimentation and so the instability appears to be continuous. Since the cycles are identical, the velocity of the top of the sedimenting region, say V, must be constant.

Although this description explains many of the features observed in the experiments, we have not yet been able to derive an exact quantitative expression for V. We have, however, using clear physical arguments been able to obtain an upper and lower bound on V; and almost all of the experimental data lie between these bounds.

It is convenient first to introduce two non-dimensional representations of the density. The first is given by

$$R = \frac{\rho_U - \rho_I}{\rho_B - \rho_I}, \tag{3.1}$$

which is a constant of each experiment and lies between 0 and 1. The second is

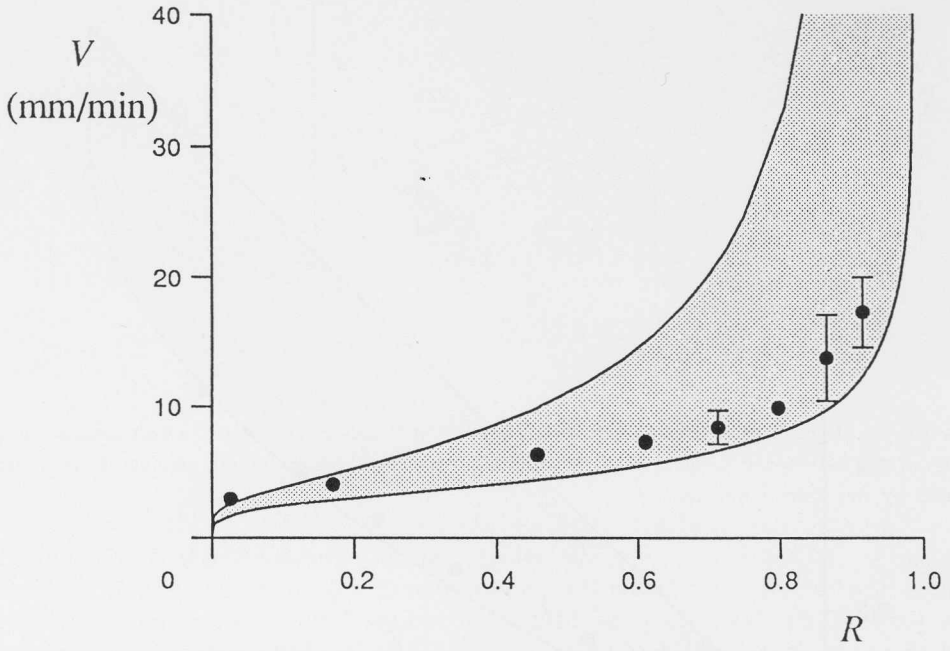

FIGURE 11. The observed interfacial velocities in experiments with type-1 particles *qua* function of the density ratio R for ρ_B = 1.059 g cm^{-3}. The error bars, where sufficiently large to be displayed, are evaluated from the variation of the interfacial position with time. The curves indicate the upper and lower bounds on the velocity determined as explained in the text.

$$r = \frac{\rho - \rho_I}{\rho_B - \rho_I}, \tag{3.2}$$

where ρ is the bulk density at any particular point in the sedimenting layer (cf. figure 10b). The function r, which is a function of the distance ζ from the top of the sedimenting interface, increases monotonically from 0 at $\zeta = 0$ to the value at the base, which is 1 or less. The function r may also be considered as a function of the Stokes free-fall velocity, v, of the particle that arrives at ζ from the top of the sedimenting layer in time t. The function $R-r$ is proportional to the local buoyancy of the suspension relative to the fluid in the upper region.

The first bound on V arises from the assertion that at least the region with positive buoyancy must rise. The buoyant region is specified by $\rho < \rho_U$, or in non-dimensional terms $r < R$. Thus a lower bound, $V_{\min}$, is given by the velocity that separates $r < R$ and $r > R$.

The second bound on V arises from the alternative assertion that at most the region with net positive buoyancy must rise. This means that the upper bound to $V, V_{\max}$, is given by

$$\int_0^{V_{\max}} [R - r(v)]dv = 0. \tag{3.3}$$

A typical graph of $V_{\min}$ and $V_{\max}$ *qua* functions of R is presented in figure 11 along with data from the relevant experiments. Further plots, for different physical parameters, are presented in Huppert *et al.* (1991) and almost all the experimental data lie within the theoretical bounds.

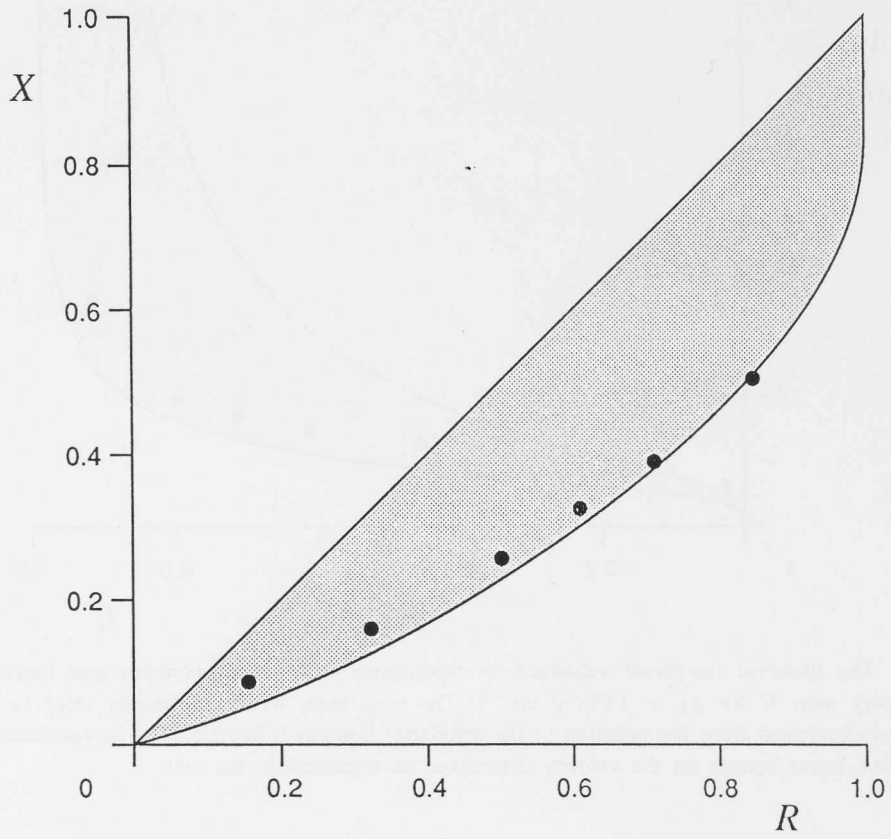

FIGURE 12. Measurements of the fraction X *qua* function of R of lifted particles in experiments with a suspension of type-2 particles with ρ_B = 1.0157 g cm^{-3}. The curves represent the upper and lower bounds predicted by the theoretical model.

A consequence of the convective mixing of the buoyant entrained region into the overlaying fluid is that some of the suspended particles are carried into the upper layer. The volume fraction X of the initial particle load of the lower layer that rises and mixes into the upper layer will be given by

$$X = \frac{1}{V}\int_0^V r(v)dv. \tag{3.4}$$

A plot of the minimum and maximum values of X, evaluated by inserting the minimum and maximum values of V in (3.4), is presented in figure 12. Also included are the experimental data obtained by decanting the upper layer immediately after the sedimentation of the lower layer had ceased and obtaining separately the weight of the lifted and deposited particles. It is seen that the data obtained agrees well with the theoretical lower bound.

While this study has uncovered a number of interesting features, there is clearly more to be understood; in particular, exactly what parameters V depends upon and how to calculate it explicitly. I and my colleagues hope to be in a position to provide some further answers in the future. For example, Ross Kerr and John Lister are currently investigating the increase of V with increasing flux Rayleigh number based on the density difference and viscosity. They are also investigating the temporal

variation of V caused by the evolution of the density of the upper layer in the case where the initial depths of the two layers are comparable.

4. Mechanically generated turbulence in a sediment layer

In this penultimate section, I should like to describe briefly some current, and still incomplete, experiments and related theory being undertaken in collaboration with Stewart Turner, during a two-month visit to Cambridge, and my Technical Officer, Mark Hallworth. Undoubtedly not all that I report will be correct. However, in well-practiced traditional style, I offer up this draft to Johnnie Miles who will scribble all over it with red pencil in a penetrating way that will allow me to proceed.

A much employed technique for studying turbulent motions, especially those in which there is a density interface, has been to use a mixing box that contains a grid of horizontal bars which are oscillated vertically. (For discussions of this technique see, for example, Turner 1979, 1986; Hannoun, Fernando & List 1988; Hannoun & List 1988; and Fernando 1991). We are employing this technique to investigate the behaviour of a sediment layer in turbulent motion beneath a clear stagnant layer; we particularly want to investigate the conditions under which all, or at least some, of the heavy particles can be held in suspension indefinitely by the mechanically generated turbulent motions.

In one series of our experiments we first filled a 30 × 8 × 30 cm high Perspex tank with a layer of water to a nominal depth of 14.0 cm. We then used the same technique described in the last section to add beneath the pure water layer a layer of carborundum particles suspended in water of the same depth. The bulk density of the suspended layer was 1.032 g cm^{-3}. A grid was constructed from a thin plate of aluminium, measuring slightly less than 30 × 8 cm, by punching out 1.0 cm square holes with a 1.5 cm spacing between the centres of the squares in the long direction. Each adjacent long row of squares was offset by 0.75 cm. The grid was oscillated with a total stroke of 2.50 cm which was centred 2.55 cm from the base. The frequency of the oscillations we have employed so far range from 0 to over 3 Hz.

We observed that as the frequency increased, each experiment attained a steady state which ranged through: all the particles being precipitated on the base; some of the particles being precipitated, while others were held in suspension; and, finally, for sufficiently high frequencies, all the particles remaining in suspension. The final thickness and particle concentration of the suspension layer, if it existed, were monitored and both were fairly strong functions of frequency.

Before discussing further details and results of the experiment, it is appropriate to present some general theoretical concepts. Consider first the situation in which no particles are precipitated. Assume further, as was observed in the experiments, that the intensity of the motion was sufficiently large for the particle concentration to be uniform ($S_t \ll 1$) and for the small variation in particle size to be irrelevant. Then the sediment layer is described entirely by its height, say h. (The concentration, say C, is then given immediately by $C = N_0/Ah$, where N_0 is the constant number of particles in the system and A is the area of the base). The behaviour of h *qua* function of time will be given by processes at the top of the sediment layer. From the long history of previous investigations, it is known that these processes involve velocities, such as entrainment velocities, horizontal velocities at the interface and Stokes settling velocities, but not accelerations or higher derivatives. Thus, mathematically, the relevant governing equations must be of the form

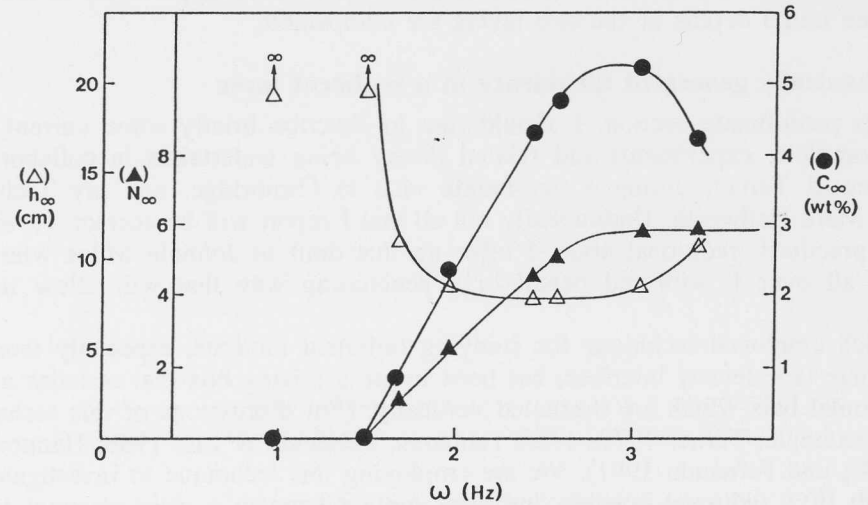

FIGURE 13. The height, h_∞, concentration, C_∞, and number of particles N_∞ at equilibrium *qua* function of ω for a mechanically driven sediment layer. The concentration is measured in wt% while the number of particles are in arbitrary units.

$$\frac{dh}{dt} = f(h,\omega;\text{geometry}), \tag{4.1}$$

$$h = h_0 \qquad (t = 0) \tag{4.2}$$

for some f, where t is the time since the initiation of the turbulent stirring, ω is the grid frequency, h_0 the initial height and 'geometry' indicates that the geometry of both the containing box and the grid is relevant. Our investigations, however, restrict attention to one particular geometry and so we will not examine its explicit influence. Note, however, we eschew the dependence of f on N_0 and h_0 on the grounds that the relationship will be derived by considering the change in height δh in time δt and the initial state of the system cannot be relevant.

Now, independent of the exact relationship for f, as $h \downarrow 0$ with ω fixed f becomes large, and will monotonically decrease as h increases, to approach $-v_S$ (the negative free-fall velocity of the particles, which will be independent of the concentration in this limit) as $h \uparrow \infty$. It follows immediately that there is one stable equilibrium point, say $h_\infty(\omega)$, which attracts all initial conditions. It can further be argued that f must be a monotonically increasing function of ω for fixed h and hence $h_\infty(\omega)$ is an increasing function of ω for the range of ω for which all the particles are held in suspension. Figure 13 presents the experimental data we have so far obtained on $h_\infty(\omega)$.

Consider now the situation in which particles can be precipitated. Then in addition to an equation analogous to (4.1), the system will be governed by an equation describing the rate of loss of particles at the base. Mathematically this means that the governing equations are of the form

$$\frac{dh}{dt} = F(h, N, \omega; \text{geometry}), \tag{4.3}$$

$$\frac{dN}{dt} = G(h, N, \omega; \text{geometry}), \tag{4.4}$$

$$h = h_0, \qquad N = N_0 \qquad (t = 0) \tag{4.5a,b}$$

for some F and G, where $N(t)$ is the total number of particles in the box, with initial value N_0. Note that in some circumstances it may be that G is constrained to be non-positive, reflecting the fact that saltation, or the lifting of particles once they have settled on the base, is impossible. (Without doubt, N cannot exceed N_0.) While it is possible to make rather vague general statements about the shape of the surfaces F and G *qua* function of h and N, it seems reasonable to say that generically the set (4.3) and (4.4) can be expected to have one, or possibly more, attractors in addition to the longtime solution $N = 0$, which lies on the boundary of the solution domain. It is seen from the experimental data plotted in figure 13 that for $\omega < 1.5 \equiv \omega_1$ in our system the energy put into the turbulent motions is not sufficient to maintain the particles in suspension and $N \downarrow 0$ as $t \uparrow \infty$. For $\omega_1 < \omega < 2.8 \equiv \omega_2$ some of the particles can be maintained permanently in suspension and both the final concentration and number of particles, C_∞ and N_∞, increases with ω while h_∞ decreases to a minimum at $\omega = 2.8$. Beyond ω_2, h_∞ increases, while C_∞ decreases because $N_\infty = N_0$ remains constant.

Figure 14 presents plots of $h(t), C(t)$ and $N(t)$ for three different values of ω, one in each of the three regimes. In all cases h is initially a decreasing function of time. For $\omega < \omega_2$, h attains a minimum and then rises monotonically, either until $N = 0$ for $\omega < \omega_1$ or until a non-zero limit is reached for $\omega_1 < \omega < \omega_2$. For $\omega_2 < \omega$, h steadily declines to a minimum, which is also the equilibrium value, as is seen in figure 14b. In all these cases $C(t)$ initially increases as the decrease in the thickness of the sediment layer dominates the decrease, if any, in the number of particles. Beyond some time it begins to decrease and either falls to zero for $\omega < \omega_1$, or to a non-zero equilibrium value for $\omega_1 < \omega$. For all values of ω, $N(t)$ is a non-increasing function of time.

We have obtained somewhat similar sets of results when sugar is added to the upper layer so that its density lies between that of the interstitial fluid and the bulk value of the lower layer. Mechanically generated turbulent motions driven from the base of the lower layer then accompany the convective motions in the upper layer driven by the release of the less dense interstitial fluid. In contrast to the sedimentation taking place in an otherwise quiescent lower layer, as described in §3, the motions in the lower layer entrain sugar from the upper layer. The density difference due to composition gradually decreases with time. Again for sufficiently low frequencies all the particles fall out, while for higher frequencies some or all the particles remain in suspension and a non-zero equilibrium value of the depth of the lower layer is reached. This cannot occur, however, until the sugar difference across the interface has become vanishingly small.

It is clear that a lot more study is needed on this problem, including the explicit evaluation of the functions f, F and G. It would also be fun to try to apply the results to some of the many natural and industrial situations in which a sediment laden fluid is in turbulent motion.

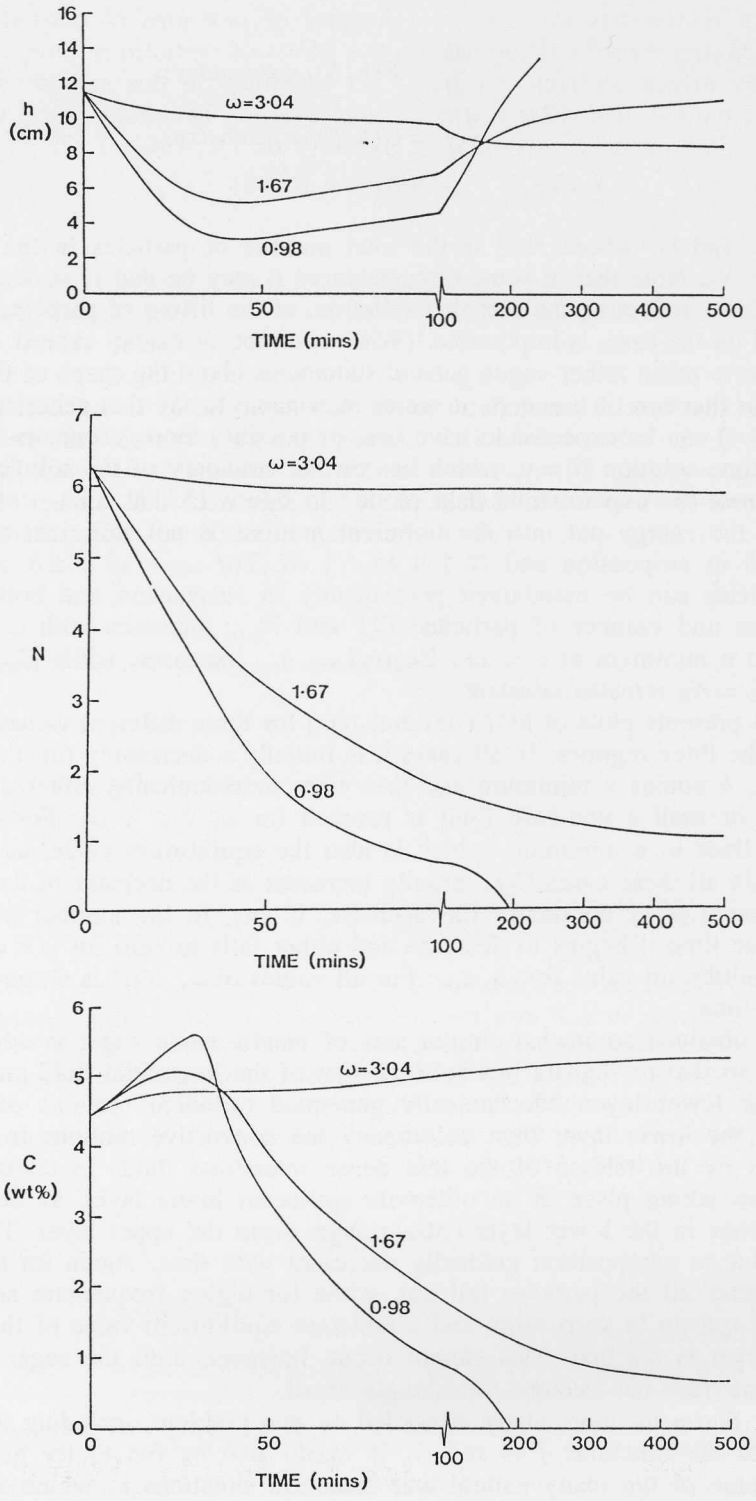

FIGURE 14. (a) The height, $h(t)$; (b) the concentration, $C(t)$; and (c) the number of particles, $N(t)$, for ω = 0.98, 1.67 and 3.04.

5. Summary

This brief review has touched on a number of problems of current interest to me. The unifying thread has been the active effect of particles on convectively and mechanically driven turbulent motions. The literature on this subject is of course large, but I believe that there are still many exciting situations to be investigated and solved. Some may be presented at meetings on December 1, 2000, 2010, ...

Acknowledgements

It is an enormous pleasure to write this article in order to help celebrate the seventieth birthday of my friend, colleague and Ph.D. supervisor, John Miles. His enthusiasm for research and for life is as powerful now as it was when we first met in 1963 and he has acted as an inspiring model for me, and I am sure many others, since that time. I am grateful to M. A. Hallworth, R. C. Kerr, T. Koyaguchi, J. R. Lister, R. S. J. Sparks and J. S. Turner, who have shared with me their ideas on particle-driven fluid flows. An earlier draft of this manuscript was improved by helpful comments from G. K. Batchelor, R. C. Kerr and J. R. Lister. My research is supported by a grant from Venture Research International, ably directed by Don Braben.

REFERENCES

DEARDORFF, J. W. & WILLIS, G. E. 1967 Investigation of turbulent thermal convection between horizontal plates. *J. Fluid Mech.* **28**, 675–704.

DENTON, R. A., & WOOD, I. R. 1979 Turbulent convection between two horizontal plates. *Int. J. Heat Mass Transfer* **22**, 1339–1346.

FERNANDO, H. J. S.1991 Turbulent mixing in stratified fluids. *Ann. Rev. Fluid Mech.* **23**, 455–493.

HANNOUN, I. A. & LIST, E. J. 1988 Turbulent mixing at a shear-free density interface. *J. Fluid Mech.* **189**, 211–234.

HANNOUN, I. A., FERNANDO, H. J. S. & LIST, E. J. 1988 Turbulence structure near a sharp density interface. *J. Fluid Mech.* **189**, 189–209.

HOWARD, L. N. 1986 Convection at high Rayleigh number. In *Proc. 11th Intl. Congr. Appl. Mech. Munich* 1109–1115, Springer.

HUPPERT, H. E. 1984 Lectures at the Woods Hole Geophysical Summer School, 1–278.

HUPPERT, H. E. & SPARKS, R. S. J. 1980 The fluid dynamics of a basaltic magma chamber replenished by influx of hot, dense ultrabasic magma. *Contrib. Min. and Petrol.* **75**, 279–289.

HUPPERT, H. E., KERR, R. C., LISTER, J. R. & TURNER, J. S. 1991 Convection and particle entrainment driven by differential sedimentation. *J. Fluid Mech.* (in press)

KOYAGUCHI, T., HALLWORTH, M. A. HUPPERT, H. E., & SPARKS, R. S. J. 1990 Sedimentation of particles from a convecting fluid. *Nature* **343**, 447–450.

MARSH, B. D. & MAXEY, M. R. 1985 On the distribution and separation of crystals in a convecting magma. *J. Volcanol. Geotherm. Res.* **24**, 95–150.

MARTIN, D. & NOKES, R. 1988 Crystal settling in a vigorously convecting magma chamber. *Nature* **332**, 534–536.

MARTIN, D. & NOKES, R. 1989 A fluid-dynamical study of crystal settling in convecting magmas. *J. Petrol.* **30**, 1471–1500.

MERRY, J. M. D. & DAVIDSON, J F. 1973 "Gulf Stream" circulation in shallow fluidised beds. *Trans. Inst. Chem. Eng.* **51**, 361–368.

STOMMEL, H. 1949 Trajectories of small bodies sinking slowly through convecting cells. *J. Mar. Res.* **8**, 24–29.

TOWNSEND, A. T. 1976 *The Structure of Turbulent Shear Flows.* Cambridge University Press.

TURNER, J. S. 1979 *Buoyancy Effects in Fluids.* Cambridge University Press.

TURNER, J. S. 1986 Turbulent entrainment: The development of the entrainment assumption, and its application to geophysical flows. *J. Fluid Mech.* **173**, 431–471.

WEINSTEIN, S. A., YUEN, D. A. & OLSEN, P. A. 1988 Evolution of crystal-settling in magma-chamber convection. *Earth Planet. Sci. Lett.* **87**, 237–248.

Mildred and Isadore Rudnick

Edwin and Melody Rood